Published in final edited form as:
Dev Dyn. 2014 October ; 243(10): 1275–1285. doi:10.1002/dvdy.24119.

Mesodermal Fgf10b cooperates with other Fgfs during induction of otic and epibranchial placodes in zebrafish.

Kirstin Maulding, **Mahesh S. Padanad**, **Jennifer Dong**, and **Bruce B. Riley***
Biology Department, Texas A&M University, College Station, TX 77843-3258

Abstract

Background—Vertebrate otic and epibranchial placodes develop in close proximity in response to localized Fgf signaling. Although less is known about epibranchial induction, the process of otic induction in highly conserved, with important roles for Fgf3 and Fgf8 reported in all species examined. Fgf10 is also critical for otic induction in mouse, but the only zebrafish ortholog examined to date, *fgf10a*, is not expressed early enough to play such a role. A second zebrafish ortholog, *fgf10b*, has not been previously examined.

Results—We find that zebrafish *fgf10b* is expressed at tailbud stage in paraxial cephalic mesoderm beneath prospective epibranchial tissue, lateral to the developing otic placode. Knockdown of *fgf10b* does not affect initial otic induction but impairs subsequent accumulation of otic cells. Formation of epibranchial placodes and ganglia are also moderately impaired. Combinatorial disruption of *fgf10b* and *fgf3* exacerbates the deficiency of otic cells and eliminates epibranchial induction entirely. Disruption of *fgf10b* and *fgf24* also strongly reduces, but does not eliminate, epibranchial induction.

Conclusions—*fgf10b* participates in a late phase of otic induction and, in combination with *fgf3*, is especially critical for epibranchial induction.

Keywords

cranial placodes; otic vesicle; epibranchial ganglia; pax2a; sox3; phox2a

INTRODUCTION

Much has been learned in recent years about developmental regulation of vertebrate cranial placodes, transient ectodermal thickenings that produce key parts of the paired sensory structures in the head. The best characterized cranial placode is the otic placode, the precursor of the inner ear. In a process that is highly conserved amongst vertebrates, the otic placode is induced near the end of gastrulation by locally expressed Fgf3 and Fgf8 (Mansour et al., 1993; Phillips et al., 2001; Léger and Brand, 2002; Maroon et al., 2002; Liu et al., 2003; Alvarez et al. 2003; Wright and Mansour, 2003; Ladher et al., 2005; Martin and Groves, 2006; Freter et al., 2008; Park and Saint-Jeannet, 2008; Padanad et al., 2012). Fgf3 is expressed in the hindbrain adjacent to the otic region, and both Fgf3 and Fgf8 are expressed in subjacent mesoderm or endoderm (Mahmood et al., 1995; Lombardo et al.,

*Communicating author: briley@bio.tamu.edu; phone 797-845-6494; fax 979-845-2891.

1998; Phillips et al., 2001; Alvarez et al., 2003; Wright et al., 2003; Ladher et al., 2005; Nechiporuk et al., 2007; Nikaido et al., 2007). In addition, in mouse Fgf10 is expressed in subjacent mesoderm and plays a critical role in otic induction (Alvarez et al., 2003; Wright and Mansour, 2003), with a similar role played by Fgf19 in chick (Ladher et al., 2000; Freter et al., 2008). Whether Fgf10 (or other Fgfs) contribute to otic induction in zebrafish has not been reported. In all species examined otic induction still occurs when any single Fgf gene is impaired, whereas impairing any two Fgf genes leads to a profound deficiency or complete loss of otic tissue. Thus redundancy provided by multiple Fgfs from multiple tissues renders the process of otic induction highly robust and resistant to perturbation.

In a developmentally related process, epibranchial placodes form in close proximity to the otic placode and produce sensory neurons of the facial, glossopharyngeal and vagal ganglia. Although epibranchial placodes are induced at a slightly later stage, they require the same Fgfs that induce the otic placode (Nechiporuk et al., 2007; Nikaido et al., 2007; Sun et al., 2007). Moreover, otic and epibranchial placodes share expression of some early markers such as *pax8* and *sox3* (Nikaido et al., 2007; Sun et al., 2007; Padanad and Riley, 2011). Otic expression of *pax8* and *sox3* occurs first, and several hours later epibranchial expression appears as an arc wrapping laterally around the otic placode. The developmental basis for the delay in epibranchial induction is not fully understood, but in zebrafish it partly reflects an additional requirement for expression of Fgf24 in the nascent otic placode (Padanad and Riley, 2011). In general, induction of epibranchial placodes appears more sensitive to loss of any one Fgf gene than does the otic placode. For example, disruption of *fgf24* has no discernable effect on otic development but causes a deficiency in all epibranchial ganglia except for the anterior-most facial ganglion (Padanad and Riley, 2011). Similarly, loss of *fgf3* alone causes only slight reduction of the otic placode but results in substantial loss of glossopharyngeal and anterior vagal ganglia (Nechiporuk et al., 2005; Nechiporuk et al., 2007). It is possible that the greater dependency of epibranchial placodes on multiple Fgf genes simply reflects their greater distance from local signaling sources.

To more fully characterize the requirements for otic and epibranchial development in zebrafish, we conducted a survey of Fgf gene expression. We report here for the first time expression of *fgf10b*, which is first detected at tailbud stage in the developing pronephros and cranial mesoderm subjacent to the prospective epibranchial ectoderm. Knockdown of *fgf10b* reduces the size of all epibranchial ganglia. Simultaneous disruption of *fgf10b* and *fgf3* blocks formation of all epibranchial ganglia. In contrast, knockdown of *fg10b* has no effect on early stages of otic induction but instead impairs a later “recruitment phase” of otic induction (Bhat et al., 2011). Accordingly, *fgf10b*-MO enhances otic deficiencies caused by disruption of either *fgf3* or *fgf8*, but does not ablate otic development altogether. Deficiencies in otic and epibranchial development caused by simultaneous knockdown of *fgf10b* and *fgf3* are rescued by low-level activation of heat shock-inducible *fgf8* from tailbud to 10-somite stage (10–14 hpf), identifying a brief window during which these Fgfs are normally required. Thus *fgf10b* plays an auxiliary role in otic induction but is especially important for epibranchial induction during early to mid-somitogenesis stages.

RESULTS

Expression of *fgf10b*

Based on conservation of function with other vertebrates, we hypothesized that an ortholog of Fgf10 is likely to contribute to otic placode induction in zebrafish. A previous study reported that the earliest cranial expression of *fgf10a* is detected at 14 hpf (10 somite stage) in the posterior lateral line (Nechiporuk and Raible, 2008), making it a poor candidate for an early otic inducer. In contrast, we found that a second ortholog, *fgf10b*, is expressed in a pattern suggesting it could play a role in otic induction. Expression of *fgf10b* is first detected at 10.7 hpf (tailbud stage) in bilateral longitudinal stripes adjacent to the hindbrain and a posterior set of stripes wrapping around the tailbud, as well as a small domain within the tailbud itself (Fig. 1A, D). The level of expression in these domains upregulates by 12 hpf (Fig. 1B, E). Co-labeling for *pax2a* and analysis of sections showed that the domain of maximal expression in the head marks paraxial cephalic mesendoderm just lateral to the developing otic placode (Fig. 1B, C). This domain predominantly marks mesodermal cells rather than endoderm, as expression was unaltered in embryos lacking endoderm due to knock down for *sox32* (*casanova*) (data not shown). The posterior domain of *fgf10b* occurs in parallel stripes of mesoderm flanking the pronephric domain of *pax2a* (Fig. 1E, F). Also appearing at 12 hpf is an additional domain of diffuse expression wrapping around the anterior neural plate (Fig. 1G). By 18 hpf, expression is limited to bilateral stripes in the head corresponding to the anterior lateral line and the developing pronephros, domains that persist through 26 hpf (Fig. 1H–J). We detected no expression at later stages (not shown).

Because expression of *Fgf10* in mouse subotic mesenchyme requires *Fgf3* and *Fgf8* (Ladher et al., 2005), we tested whether there is a similar requirement for zebrafish *fgf10b*. Expression of *fgf10b* appeared normal in *fgf3* morphants but was markedly reduced in the posterior limit of the cranial domain in *fgf8* morphants and was almost undetectable in *fgf3-fgf8* double morphants (Fig. 1K–M). Thus expression of *fgf10b* adjacent to prospective otic/epibranchial tissue requires prior expression of *fgf3* and *fgf8*, similar to the regulation seen in mouse.

Testing morpholinos for *fgf10b*

We next tested three different morpholino oligomers (MOs) to knockdown *fgf10b* function, one to block translation and two to block splicing at different exon-intron junctions (Fig. 2A). Injection of 5 ng of individual MOs caused similar phenotypes, although the translation blocker caused moderate non-specific cell death in the brain, a phenotype often associated with off-target effects (not shown). The effects of splice-blocking MOs appeared more specific and showed little or no brain necrosis. To further minimize the risk of potential off-target effects all data reported herein were generated by co-injecting 2.5 ng of each splice-blocker. This combination effectively and specifically reduced accumulation of mature *fgf10b* mRNA (Fig. 2B) and caused a highly reproducible phenotype with little or no cell death in the brain (Fig. 3A, D).

Role in otic placode induction

Knockdown of *fgf10b* resulted in development of a ventrally curved embryonic axis and, additionally, the circumference of the otic vesicle was reduced by 10–15% at 27 hpf ($p<.05$) (Fig. 3D, E). Examination of early otic markers showed that knockdown of *fgf10b* had no affect on the pattern of *pax8* expression at 11 hpf (not shown). By 14 hpf, however, the otic domain of *pax2a* was reduced in area by about 10% in *fgf10b* morphants ($p<.05$) (Fig. 3F). Thus, *fgf10b* is not required for initial induction of *pax8* but is instead required for subsequent expansion of the otic domain. This is consistent with the slightly later onset of *fgf10b* expression relative to early otic expression of *pax8*.

We hypothesized that redundancy from other inductive Fgfs partially compensates for loss of *fgf10b*. In support, loss of *fgf8* caused a 65–70% reduction in the size of the otic placode and vesicle (Fig. 3H, I) and there was a slight additional decrease (though not statistically significant) following knockdown of *fgf10b* in $fgf8^{-/-}$ mutants (Fig. 3K, L). Knockdown of *fgf10b* also enhanced the short axis defect seen in $fgf8^{-/-}$ mutants (Fig. 3G, J). Because the severity of the $fgf8^{-/-}$ mutant phenotype complicates analysis of *fgf10b* function, we also examined the interaction between *fgf10b* and *fgf3*. Loss of *fgf3* alone caused only 5% reduction in the size of the otic placode and vesicle (Fig. 3N, O), whereas disruption of both *fgf3* and *fgf10b* reduced the size of the otic placode and vesicle by 25–30% (Fig. 3Q, R). This is significantly more severe than the phenotype seen in *fgf10b* morphants (*pax2a* domain, $p<.01$). These findings are consistent with a model in which *fgf3* and *fgf8* are required for initial otic induction whereas *fgf10b* is required only to increase the size of the otic placode after 11 hpf (see Discussion).

The deficiency in otic tissue caused by knockdown of *fgf10b* could arise from insufficient induction of otic cells or failure to maintain otic fate. To distinguish between these possibilities, we determined the number of *pax2a*-expressing cells at stages after *fgf10b* is normally expressed. Staining of otic cells with Pax2 polyclonal antibody is first detected at around 12 hpf, indicating a lag of roughly 1 hour from the onset of *pax2a* transcription. At 12 hpf the number of Pax2-positive cells appeared normal in embryos knocked down for *fgf10b* and/or *fgf3* (Fig. 4A). We previously documented that the number of Pax2-positive cells shows a 50% increase between 12 hpf and 14 hpf (10 somites) through a recruitment process that does not require cell division (Riley et al. 2010; Bhat et al., 2011). The same fold-increase is seen in *fgf3* morphants, while *fgf10b* morphants show a 35% increase by 14 hpf (Fig. 4A). In contrast, there is no detectable change in the number of Pax2-positive cells in *fgf3-fgf10b* double morphants by 14 hpf (ig. 4A). This failure in otic expansion does not reflect attrition from elevated cell death, as the number of acridine orange-staining cells is normal in *fgf3-fgf10b* double morphants during this period (Fig. 4C–E). We next tested whether the deficiency in otic expansion seen in *fgf3-fgf10b* double morphants could be rescued by weakly elevating Fgf signaling after the initial phase of otic induction. For this we used a heat shock-inducible transgene, *hs:fgf8*, activated at a low level by mild heat shock at 35°C. Under these conditions it takes about 1 hour to detect a rise in Fgf signaling (not shown). Unlike standard heat shock conditions at 39°C (Padanad et al., 2012), incubating *hs:fgf8/+* embryos at 35°C beginning at 10 hpf did not significantly enhance otic development (Fig. 4B). Nevertheless, weak activation of *hs:fgf8* at 35°C was sufficient to

rescue the otic deficiency in *fgf3-fgf10b* double morphants (Fig. 4B). Together these data indicate that *fgf10b*, acting together with *fgf3*, is required for a late secondary phase of otic induction.

To test whether the early requirement for *fgf10b* affects subsequent otic patterning, we examined expression of regionally expressed markers within the developing otic vesicle. *fgf10b* morphants showed normal expression of all markers tested, including anterior marker *pax5*, posterior marker *pou3f3b* (*zp23*), dorsal marker *dlx3b* and ventrolateral marker *otx1b* (Fig. 5A, B). In *fgf3-fgf10b*-deficient embryos, *dlx3b* and *otx1b* were expressed normally, whereas *pax5* expression was lost and the domain of *pou3f3b* expanded anteriorly (Fig. 5A–D). Altered expression of *pax5* and *pou3f3b* was also seen in *fgf3*$^{-/-}$ mutants (Fig. 5A, B), reflecting the role of *fgf3* in regulating antero-posterior patterning in the otic vesicle (Kwak et al., 2002; Kwak et al., 2006; Hammond and Whitfield, 2011). Despite the changes in patterning in *fgf3-fgf10b*-deficient embryos, sensory epithelia and neurons of the statoacoustic ganglion (SAG) appeared to form relatively normally, albeit in slightly smaller domains corresponding to the reduced size of the otic vesicle (Fig. 5E, F). Thus, knockdown of *fgf10b* does not cause obvious changes in otic patterning despite the early deficiency in otic placode development. Moreover, altered patterning seen in *fgf3-fgf10b*-deficient morphants is attributable solely to loss of *fgf3*.

Role in epibranchial placode induction

Epibranchial placodes, which produce sensory neurons of epibranchial ganglia, are produced in close proximity to the otic placode and are co-regulated in part by mesodermal expression of *fgf3* (Nechiporuk et al., 2007). We therefore examined whether *fgf10b* cooperates with *fgf3* in epibranchial regulation. Knockdown of *fgf10b* alone caused reduction in all epibranchial ganglia, as marked by reduced domains of *phox2a* at 36 hpf (Fig. 6A, C). As previously reported (Nechiporuk et al., 2007), disruption of *fgf3* resulted in loss of glossopharyngeal and vagal I ganglia and reduction in the facial ganglion (Fig. 6E). Embryos deficient for both *fgf3* and *fgf10b* produced little or no epibranchial ganglia (Fig. 6G). To determine the developmental basis for loss of epibranchial ganglia, embryos were examined for expression of *sox3*, the earliest known marker of epibranchial placode formation (Nikaido et al., 2007; Sun et al., 2007). In control embryos expression of *sox3* is initially co-induced with *pax8* in the otic placode by 9.5–10 hpf. Between 11–12 hpf, *sox3* expression expands outward to mark adjacent epibranchial tissue and simultaneously downregulates in otic tissue. Knockdown of *fgf10b* did not affect otic expression of *sox3* at 11 hpf, but the epibranchial domain of *sox3* appeared slightly reduced at 13 hpf ($p<.05$) (Fig. 6B, D). A slight but insignificant reduction in the epibranchial domain of *sox3* was also seen in *fgf3* morphants or mutants (Fig. 6F). In contrast, the epibranchial domain of *sox3* was reduced by half in *fgf3-fgf10b* double morphants (Fig. 6H), a highly significant reduction relative to *fgf10b* morphants ($p<.01$).

To confirm the early deficiency in epibranchial placode formation, we examined expression of *pax2a* at 24 hpf when epibranchial placode thickening first becomes evident. As expected, moderate deficiencies were seen in the epibranchial domain of *pax2a* in *fgf3* morphants and *fgf10b* morphants, and this domain was almost completely ablated in *fgf3-*

fgf10b double morphants (Fig. 7). Thus, *fgf10b* and *fgf3* are together required for proper induction of epibranchial placodes and subsequent differentiation of epibranchial ganglia.

To examine the temporal requirements for Fgf in epibranchial placode induction, we tested whether weak early activation of *hs:fgf8* could rescue the epibranchial deficiency in *fgf3-fgf10b* double morphants. Incubation of *hs:fgf8*/+ transgenic embryos at 35°C from 10 hpf until 8- or 10-somite stage (equivalent to 13 or 14 hpf, respectively) had negligible effects on placodal expression of *pax2a* or *sox3*, nor was development of epibranchial ganglia significantly altered at 36 hpf (Fig. 8G–I). Nevertheless, this brief pulse of *hs:fgf8* activity was sufficient to fully rescue otic development and provide substantial rescue of epibranchial development in *fgf3-fgf10b* double morphants (compare Fig. 8D–F, J–L). Similar rescue was obtained by activating *hs:fgf8* at 37°C from 12 to 14 hpf (data not shown). Rescue of epibranchial neurogenesis was not complete, however (Fig. 8L), probably reflecting a later requirement for *fgf3* expressed in pharyngeal endoderm at 24 hpf (Nechiporuk et al., 2005). Nevertheless rescue by early *hs:fgf8* activity suggests that *fgf10b* and *fgf3* are required during early somitogenesis stages for epibranchial placode induction.

Because epibranchial placode development also partly depends on expression of *fgf24* in the otic placode (Padanad and Riley, 2011), we examined genetic interaction between *fgf24* and *fgf10b*. As previously reported (Padanad and Riley, 2011), knockdown of *fgf24* caused a deficiency of glossopharyngeal and vagal ganglia at 36 hpf, whereas the facial ganglion developed normally (Fig. 6I). Note, the deficiency seen in posterior epibranchial ganglia is less severe than what we previously reported at 30 hpf (Padanad and Riley, 2011), indicating that *fgf24* morphants show partial recovery by 36 hpf. Knockdown of both *fgf10b* and *fgf24* led to a more pronounced deficiency of glossopharyngeal and vagal ganglia at 36 hpf than was seen in single morphants (compare Fig. 6C, I, K). The deficiencies in epibranchial ganglia seen at 36 hpf reflected corresponding deficiencies in the area of *sox3* expression seen at 13 hpf (Fig. 6J, L). Specifically, knockdown of *fgf24* caused a decrease of nearly a 20% in the *sox3* domain ($p<.01$), and *fgf10b-fgf24* double morphants showed a decrease of about 30% ($p<.01$). Thus, *fgf10b* and *fgf24* work together to induce a normal amount of epibranchial tissue.

No role in more anterior placodes

Because *fgf10b* expression extends into more anterior mesoderm, we examined whether more anterior placodes were affected by knockdown of *fgf10b*. Expression of *neurod* marks early stages of development of the anterior lateral line and trigeminal placodes at 14 hpf, and these domains appeared normal in *fgf10b* morphants (Fig. 9A, B). Similarly, *neurod* expression was normal in *fgf3* and *fgf3-fgf10b* double morphants (Fig. 9C, D). We also noted that nasal pit and the lens of the eye form with normal morphology in embryos disrupted for *fgf3* and/or *fgf10b* (not shown). Thus, only the otic and epibranchial placodes require *fgf10b* and *fgf3* for proper development.

DISCUSSION

We have shown that *fgf10b* is expressed in cranial paraxial mesoderm by tailbud stage and contributes to induction of both otic and epibranchial placodes (Fig. 10). As detailed below,

our findings complement and extend earlier studies and shed light on evolutionary conservation of the underlying mechanisms. We also document expression of *fgf10b* in mesoderm flanking the developing pronephros but did not investigate the function of *fgf10b* in this domain.

Otic induction

The principal otic inducers in zebrafish are Fgf3 and Fgf8 secreted from the hindbrain and subotic mesendoderm (Fig. 10A). Accordingly, disruption of both *fgf3* and *fgf8* abolishes otic induction entirely (Phillips et al., 2001; Léger and Brand, 2002; Maroon et al., 2002; Liu et al., 2003). In contrast, *fgf10b* is expressed after the initial phase of otic induction such that knockdown of *fgf10b* results in only 10–15% reduction in the size of the otic placode and vesicle (Fig. 3). This change is consistent with a role for *fgf10b* in "secondary otic recruitment" (Fig. 10B). We previously documented that the otic placode continues to expand after 11 hpf through a mechanism that does not involve cell division (Riley et al., 2010). Instead, during the later phase of recruitment cells converge by directed migration from surrounding regions into the growing otic placode, a process that requires *integrin-α5* (*itga5*) (Bhat et al., 2011). In *itga5* mutants, cells meander haphazardly such that fewer cells move into range of inductive signals in time to join the otic placode. Time-lapse imaging of lineage-labeled cells shows that secondary otic recruitment occurs during a window from 11–12.5 hpf (Bhat et al., 2011). This is consistent with the timing of *fgf10b* expression. Moreover, the domain of *fgf10b* expression is optimally positioned to impact late-migrating cells just prior to entering the otic domain (Fig. 1A, 10B). We do not know whether disruption of *fgf10b* affects the pattern of cell migration, but it clearly impedes later expansion of the otic domain. Mesodermal Fgf3 also appears to contribute to secondary otic recruitment, as *fgf3-fgf10b* double morphants show a significantly more pronounced otic deficiency than single morphants, and this deficiency is rescued by a weak pulse of *hs:fgf8* activity beginning after initial otic induction (Figs. 3, 4).

Comparison between mouse and zebrafish suggests a broadly conserved role for Fgf10 in otic development. In a pattern similar to zebrafish *fgf10b*, mouse *Fgf10* is first expressed in cranial mesoderm beneath the prospective otic placode at the zero-somite stage and requires earlier expression of *Fgf8* (Ladher et al. 2005). The mesodermal domain of *Fgf10* is clearly important for otic induction in mouse (Alvarez at el., 2003; Wright and Mansour, 2003). Subsequently, mouse *Fgf10* is expressed in the developing otic vesicle where it regulates neurogenesis (Pauley et al., 2003). In zebrafish, comparable expression in the otic vesicle is observed for *fgf10a* but not *fgf10b* (Feng and Xu, 2010). Thus the two *fgf10* paralogs in zebrafish appear to have undergone subfunctionalization to regulate early vs. late functions in otic development. In chick *Fgf10* is first detected in the otic placode and vesicle to regulate otic neurogenesis (Alsina et al., 2004), but no earlier mesodermal domain has been detected. Instead, mesodermal expression of *Fgf19* contributes to otic induction in chick (Ladher et al., 2000), a function not shared by *Fgf19* orthologs in zebrafish or mouse (Wright et al., 2004; Miyake et al., 2005).

Epibranchial induction

The role of Fgf in epibranchial induction has been studied most extensively in zebrafish. Early markers of epibranchial induction include *sox3*, *pax8* and *pax2a*, all of which require Fgf (Nikaido et al., 2007; Sun et al., 2007; Padanad et al., 2011; McCarroll et al., 2012). Expression of *sox3* is particularly dynamic and expands from a central otic domain into adjacent epibranchial tissue between 11 and 12 hpf. Time lapse imaging of cell migration shows that cells continue to enter the epibranchial domain of *pax2a* expression until just after 13 hpf (Bhat et al., 2011; Fig. 10C). Timed disruption of Fgf using the pharmacological inhibitor SU5402 reveals that epibranchial induction follows an anterior-to-posterior progression: Induction of the facial placode requires Fgf by around11.5 hpf whereas induction of glossopharyngeal and vagal placodes require Fgf at slightly later stages (Nechiporuk et al., 2007). The above studies suggest a general timeframe for epibranchial induction that is consistent with the requirement for Fgf3 and Fgf10b. Nearly all epibranchial development is abolished in *fgf3-fgf10b* deficient embryos, and this deficiency is substantially rescued by a low pulse of *hs:fgf8* activity at 35°C from 10–14 hpf (Figs. 3 and 8) or a moderate pulse at 37°C from 12–14 hpf (data not shown). In addition, Fgf24 secreted from the nascent otic placode during the same timeframe is required for normal development of gossopharyngeal and vagal placodes (Padanad et al., 2011; Fig. 6; Fig. 10C). Interestingly, otic *fgf24* is expressed relatively normally in *fgf3-fgf10b* deficient embryos yet is not sufficient to support epibranchial induction. Thus epibranchial induction is critically dependent on the spatial distribution and overall level of Fgf signaling during early somitogenesis stages.

In addition to its early inductive role, *fgf3* is also expressed at later stages in pharyngeal endoderm and helps initiate neurogenesis within developing epibranchial tissue (Nechiporuk et al., 2005). Blocking endoderm formation does not block induction of *sox3* in nascent epibranchial placodes but profoundly affects subsequent neurogenesis. Thus, loss of *fgf3* affects both epibranchial induction and later neurogenesis, compounding its interaction with *fgf10b*. Pharyngeal Bmp is also required for epibranchial neurogenesis (Begbie et al., 1999; Holzschuh et al., 2005), although the relationship between pharyngeal Fgf3 and Bmp is not known.

Studies in other vertebrates on the role of Fgf in epibranchial induction are still limited. The earliest potential marker for epibranchial development in chick and mouse is *Foxi2*, which is expressed in ectoderm immediately surrounding the nascent otic placode and likely encompasses epibranchial precursors (Oyama and Groves, 2004; Freter et al., 2008). Expression of chick *Foxi2* requires Fgf and increases in response to exogenous Fgf2 (Freter et al., 2008; Yang et al., 2013), but there have been no knockdown studies to indicate which endogenous *Fgf* genes are involved. The situation in mouse is less clear, as the epibranchial domain of *Foxi2* expands at the expense of otic markers in *Fgf3-Fgf10* double mutants (Urness et al., 2010). Clearly additional studies are needed to clarify these issues and to evaluate the degree to which mechanisms have been conserved in various vertebrate species.

EXPERIMENTAL PROCEDURES

Fish Strains and Staging

Wild-type zebrafish were obtained from that AB line (Eugene, OR). Embryos were developed under standard conditions at 28.5°C and staged according to standard morphological criteria (Kimmel et al., 1995). To ensure precise staging of young embryos used for gene expression studies, embryos were co-stained for *myoD* to count somites. Mutant alleles *fgf3*^{t26212} and *fgf8*^{x15} and PCR-based genotyping protocols have been previously described (Herzog et al., 2004; Kwon and Riley, 2009). Transgenic lines *TG(brn3c:gap43-GFP)* (Xiao et a., 2005) and *TG(-17.6isl2b:GFP)*^{zc7} (Pitman et al., 2008) were used to visualize sensory hair cells and mature neurons of the statoacoustic ganglion, respectively. Misexpression of *fgf8* was achieved by briefly heat shocking heterozygous transgenic embryos carrying *Tg(hsp70:fgf8)*^{x17} (Millimaki et al., 2010) at 35°C.

Morpholinos and Phenotypic Analysis

Morpholino oligomers (MOs) were obtained from Gene Tools, Inc. Sequences and testing of MOs to knockdown *fgf3, fgf8, fgf24, p53* and *casanova* (*sox32*) have been previously described (Draper et al., 2001; Sakaguchi et al., 2001; Fischer et al., 2003; Robu et al., 2007; Kwon and Riley, 2009). To knockdown *fgf10b*, the following MO sequences were used: tb-MO to block translation TCCATCTCCTCATGGTACTCCTCAT; e1i1-MO to target the exon1-intron1 splice junction AATCGTGACTCACTGTACGGGTCGT; e2i2-MO to target the exon2-intron2 splice junction GACACTCACCACTCCAAACAGCTCC. For most target sequences, embryos were injected with 5ng per MO at the one-cell stage. All three *fgf10b*-MOs produced similar phenotypes. For most experiments involving knockdown of *fgf10b*, embryos were co-injected with 2.5ng each of e1i1-MO and e2i2-MO to minimize off-target effects. To further guard against nonspecific cell death caused from off-target effects, embryos were also co-injected with *p53*-MO (Robu et al., 2007), which did not detectably alter the phenotypes reported herein. Interactions with *fgf3* were conducted initially with *fgf3*-MO and confirmed in *fgf3* mutants. Phenotypes described herein were assessed with at least 20 specimens per time point and probe. Quantification of otic vesicles size (area presented in lateral views) and gene expression areas was performed using Photoshop. Areas presented in figures were normalized relative to wild-type control embryos and indicate the mean ± standard deviation of 8–10 specimens. Where indicated, statistical significance was evaluated using students' t-test or, where appropriate, ANOVA and Tukey post-hoc HSD tests.

PCR

Efficacy of *fgf10b* splice-blocking MOs was evaluated at 12 hpf by RT-PCR using the following primers: sense 5'-GAT GGA CAG TGA GTA AGA GTG TGT-3'; antisense 5'-TTC TCC TCG ATG CGC TCC TTC A-3'. The *fgf10b* sequence was amplified through 36 cycles with an annealing temperature of 64°C. Amplification of *ornithine decarboxylase* (*odc*) was used as a control.

Gene expression, cell death and Sectioning

Gene expression patterns were visualized by whole-mount in situ hybridization or staining with Pax2 polyclonal antibody (Covance, 1:100 dilution) as previously described (Phillips et al., 2001). For tissue sections, embryos were embedded in Immunobed resin (Polysciences No. 17324) and cut into 7 μm sections. Cell death was visualized by incubating live dechorionated embryos in acridine orange as previously described (Millimaki et al., 2010).

Acknowledgments

Grant support: NIDCD R01-DC03806.

REFERENCES

Alsina B, Abello G, Ulloa E, Henrique D, Pujades C, Giraldez F. FGF signaling is required for determination of otic neuroblasts in the chick embryo. Dev. Bio. 2004; 267:119–134. [PubMed: 14975721]

2. Alvarez Y, Alonso MT, Vendrell V, Zelarayan LC, Chamero P, Theil T, Bosl MR, Kato S, Maconochie M, Riethmacher D. Requirements for FGF3 and FGF10 during inner ear formation. Development. 2003; 130:6329–6338. [PubMed: 14623822]

3. Begbie J, Brunet JF, Rubenstein JLR, Graham A. Induction of the epibranchial placodes. Development. 1999; 126:895–902. [PubMed: 9927591]

4. Bhat N, Riley BB. Integrin-α5 coordinates assembly of posterior cranial placodes in zebrafish and enhances Fgf-dependent regulation of otic/epibranchial cells. PLoS ONE. 2011; 6(12):e27778. [PubMed: 22164214]

5. Draper BW, Morcos PA, Kimmel CB. Inhibition of zebrafish *fgf8* pre-mRNA splicing with morpholino oligos: A quantifiable method for gene knockdown. Genesis. 2001; 30:154–156. [PubMed: 11477696]

6. Feng Y, Xu Q. Pivotal role of *hmx2* and *hmx3* in zebrafish inner ear and lateral line development. Dev Biol. 2010; 339:507–518. [PubMed: 20043901]

7. Fischer S, Draper BW, Neumann CJ. The zebrafish *fgf24* mutant identifies an additional level of Fgf signaling involved in vertebrate forelimb initiation. Development. 2003; 130:3515–3524. [PubMed: 12810598]

8. Freter S, Muta Y, Mak SS, Rinkwitz S, Ladher RK. Progressive restriction of otic fate: the role of FGF and Wnt in resolving inner ear potential. Development. 2008; 135:3415–3424. [PubMed: 18799542]

9. Hammond KL, Whitfield TT. Fgf and Hh signaling act on a symmetrical pre-pattern to specify anterior and posterior identity in the zebrafish otic placode and vesicle. Development. 2011; 138:3977–3987. [PubMed: 21831919]

10. Herzog W, Sonntag C, von der Hardt S, Roehl HH, Varga ZM, Hammerschmidt M. Fgf3 signaling from the ventral diencephalon is required for early specification and subsequent survival of the zebrafish adenohypophysis. Development. 2004; 131:3681–3692. [PubMed: 15229178]

11. Holzschuh Y, Wada N, Wada C, Schaffer A, Javidan Y, Tallafuß A, Bally-Cuif L, Schilling TF. Requirements for endoderm and BMP signaling in sensory neurogenesis in zebrafish. Development. 2005; 132:3731–3742. [PubMed: 16077092]

12. Kimmel CB, Ballard WW, Kimmel SR, Ullmann B, Schilling TF. Stages of embryonic development of the zebrafish. Dev Dyn. 1995; 203:253–310. [PubMed: 8589427]

13. Kwak SJ, Phillips BT, Heck R, Riley BB. An expanded domain of *fgf3* expression in the hindbrain of zebrafish *valentine* mutants results in mis-patterning of the otic vesicle. Development. 2002; 129:5279–5287. [PubMed: 12399318]

14. Kwak SJ, Vemaraju S, Moorman SJ, Zeddies D, Popper AN, Riley BB. Zebrafish *pax5* regulates development of the utricular macula and vestibular function. Dev Dyn. 2006; 235:3026–3038. [PubMed: 17013878]

15. Kwon HJ, Riley BB. Mesendodermal signals required for otic induction: Bmp-antagonists cooperate with fgf and can facilitate formation of ectopic otic tissue. Dev Dyn. 2009; 238:1582–1594. [PubMed: 19418450]
16. Ladher RK, Anakwe KU, Gurney AL, Schoenwolf GC, Francis-West PH. Identification of synergistic signals initiating inner ear development. Science. 2000; 290:1965–1968. [PubMed: 11110663]
17. Ladher RK, Wright TJ, Moon AM, Mansour SL, Schoenwolf GC. FGF8 initiates inner ear induction in chick and mouse. Genes Dev. 2005; 19:603–613. [PubMed: 15741321]
18. Léger S, Brand M. Fgf8 and Fgf3 are required for zebrafish ear placode induction, maintenance and inner ear patterning. Mech Dev. 2002; 119:91–108. [PubMed: 12385757]
19. Liu D, Chu H, Maves L, Yan YL, Morcos PA, Postlethwait JH, Westerfield M. Fgf3 and Fgf8 dependent and independent transcription factors are required for otic placode specification. Development. 2003; 130:2213–2224. [PubMed: 12668634]
20. Lombardo A, Isaacs HV, Slack JMW. Expression and functions of FGF-3 in Xenopus development. Dev Dyn. 1998; 212:75–85. [PubMed: 9603425]
21. Mahmood R, Kiefer P, Guthrie S, Dickson C, Mason I. Multiple roles for FGF-3 during cranial neural development in the chicken. Development. 1995; 121:1399–1410. [PubMed: 7789270]
22. Mansour SL, Goddard JM, Capecchi MR. Mice homozygous for a targeted disruption of the proto-oncogene *int-2* have developmental defects in the tail and inner ear. Development. 1993; 117:13–28. [PubMed: 8223243]
23. Maroon H, Walshe J, Mahmood R, Kiefer P, Dickson C, Mason I. Fgf3 and Fgf8 are required together for formation of the otic placode and vesicle. Development. 2002; 129:2099–2108. [PubMed: 11959820]
24. Martin K, Groves AK. Competence of cranial ectoderm to respond to Fgf signaling suggests a two-step model of otic placode induction. Development. 2006; 133:877–887. [PubMed: 16452090]
25. McCarroll MN, Lewis ZR, Culbertson MD, Martin BL, Kimelman D, Nechiporuk AV. Graded levels of Pax2a and Pax8 regulate differentiation during sensory placode formation. Development. 2012; 139:2740–2750. [PubMed: 22745314]
26. Millimaki BB, Sweet EM, Riley BB. Sox2 is required for maintenance and regeneration, but not initial development, of hair cells in the zebrafish inner ear. Dev Biol. 2010; 338:262–269. [PubMed: 20025865]
27. Miyake A, Nakayama Y, Konishi M, Itoh N. *Fgf19* regulated by Hh signaling is required for zebrafish forebrain development. Dev Biol. 2005; 288:259–275. [PubMed: 16256099]
28. Nechiporuk A, Raible DW. FGF-dependent mechanosensory organ patterning in zebrafish. Science. 2008; 320:1774–1777. [PubMed: 18583612]
29. Nechiporuk A, Linbo T, Raible DW. Endoderm-derived Fgf3 is necessary and sufficient for inducing neurogenesis in the epibranchial placodes in zebrafish. Development. 2005; 132:3717–3730. [PubMed: 16077091]
30. Nechiporuk A, Linbo T, Poss KD, Raible DW. Specification of epibranchial placodes in zebrafish. Development. 2007; 134:611–623. [PubMed: 17215310]
31. Nikaido M, Doi K, Shimizu T, Hibi M, Kikuchi Y, Yamasu K. Initial specification of the epibranchial placode in zebrafish embryos depends on the fibroblast growth factor signal. Dev Dyn. 2007; 236:564–571. [PubMed: 17195184]
32. Ohyama T, Groves AK. Expression of mouse Foxi1 class genes in early craniofacial development. Dev Dyn. 2004; 231:640–646. [PubMed: 15376323]
33. Padanad MS, Riley BB. Pax2a proteins coordinate sequential induction of otic and epibranchial placodes through differential regulation of *foxi1*, *soxi3*, and *fgf24*. Dev Biol. 2011; 351:90–98. [PubMed: 21215261]
34. Padanad MS, Bhat N, Guo B, Riley BB. Conditions that influence the response to Fgf during otic placode induction. Dev Biol. 2012; 364:1–10. [PubMed: 22327005]
35. Park BY, Saint-Jeannet JP. Hindbrain-derived Wnt and Fgf signals cooperate to specify the otic placode in *Xenopus*. Dev Biol. 2008; 324:108–121. [PubMed: 18831968]
36. Pauley S, Wright TJ, Pirvola U, Ornitz D, Beisel K, Fritzsch B. Expression and function of FGF10 in mammalian inner ear development. Dev Dyn. 2003; 227:203–215. [PubMed: 12761848]

37. Pittman AJ, Law MY, Chien CB. Pathfinding in a large vertebrate axon tract: isotypic interactions guide retinotectal axons at multiple choice points. Development. 2008; 135:2865–2871. [PubMed: 18653554]
38. Phillips BT, Bolding K, Riley BB. Zebrafish *fgf3* and *fgf8* Encode Redundant Functions Required for Otic Placode Induction. Dev Biol. 2001; 235:351–365. [PubMed: 11437442]
39. Riley BB, Sweet EM, Heck R, Evans A, McFarland KN, Warga RM, Kane DA. Characterization of *harpy/Rca1/emi1* mutants: Patterning in the absence of cell division. Dev Dyn. 2010; 239:828–843. [PubMed: 20146251]
40. Robu ME, Larson JD, Nasevicius A, Beiraghi S, Brenner C, Farber SA, Ekker SC. p53 activation by knockdown technologies. PLoS Genetics. 2007; 3(%):e78. [PubMed: 17530925]
41. Sakaguchi T, Kuroiwa A, Takeda H. A novel sox gene *226D7*, acts downstream of Nodal signaling to specify endoderm precursors in zebrafish. Mech Dev. 2001; 107:25–38. [PubMed: 11520661]
42. Sun SK, Dee CT, Tripathi VB, Rengifo A, Hirst CS, Scotting PJ. Epibranchial and otic placodes are induced by a common Fgf signal, but their subsequent development is independent. Dev Biol. 2007; 303:675–686. [PubMed: 17222818]
43. Urness LD, Paxton CN, Wang X, Schoenwolf GC, Mansour SL. FGF signaling regulates otic placode induction and refinement by controlling both ectodermal target genes and hindbrain *Wnt8c*. Dev Biol. 2010; 340:595–604. [PubMed: 20171206]
44. Wright TJ, Mansour SL. Fgf3 and Fgf10 are required for mouse otic placode induction. Development. 2003; 130:3379–3390. [PubMed: 12810586]
45. Wright TJ, Ladher R, McWhirter J, Murre C, Schoenwolf GC, Mansour SL. Mouse FGF15 is the ortholog of human and chick FGF19, but is not uniquely required for otic induction. Dev Biol. 2004; 269:264–275. [PubMed: 15081372]
46. Xiao T, Roeser T, Staub W, Baier H. A GFP-based genetic screen reveals mutations that disrupt the architecture of the zebrafish retinotectal projection. Development. 2005; 132:2955–2967. [PubMed: 15930106]
47. Yang L, O'Neill P, Martin K, Maass JC, Vassilev V, Ladher R, Groves AK. Analysis of FGF-dependent and FGF-independent pathways in otic placode induction. PLoS ONE. 2013; 8(1):e55011. [PubMed: 23355906]

Key Findings

Fgf10b is required for a late phase of otic induction, accounting for 10–15% of the otic placode.

Fgf10b plus Fgf3 are absolutely required for epibranchial induction.

Fgf10b also cooperates with Fgf24 in epibranchial induction.

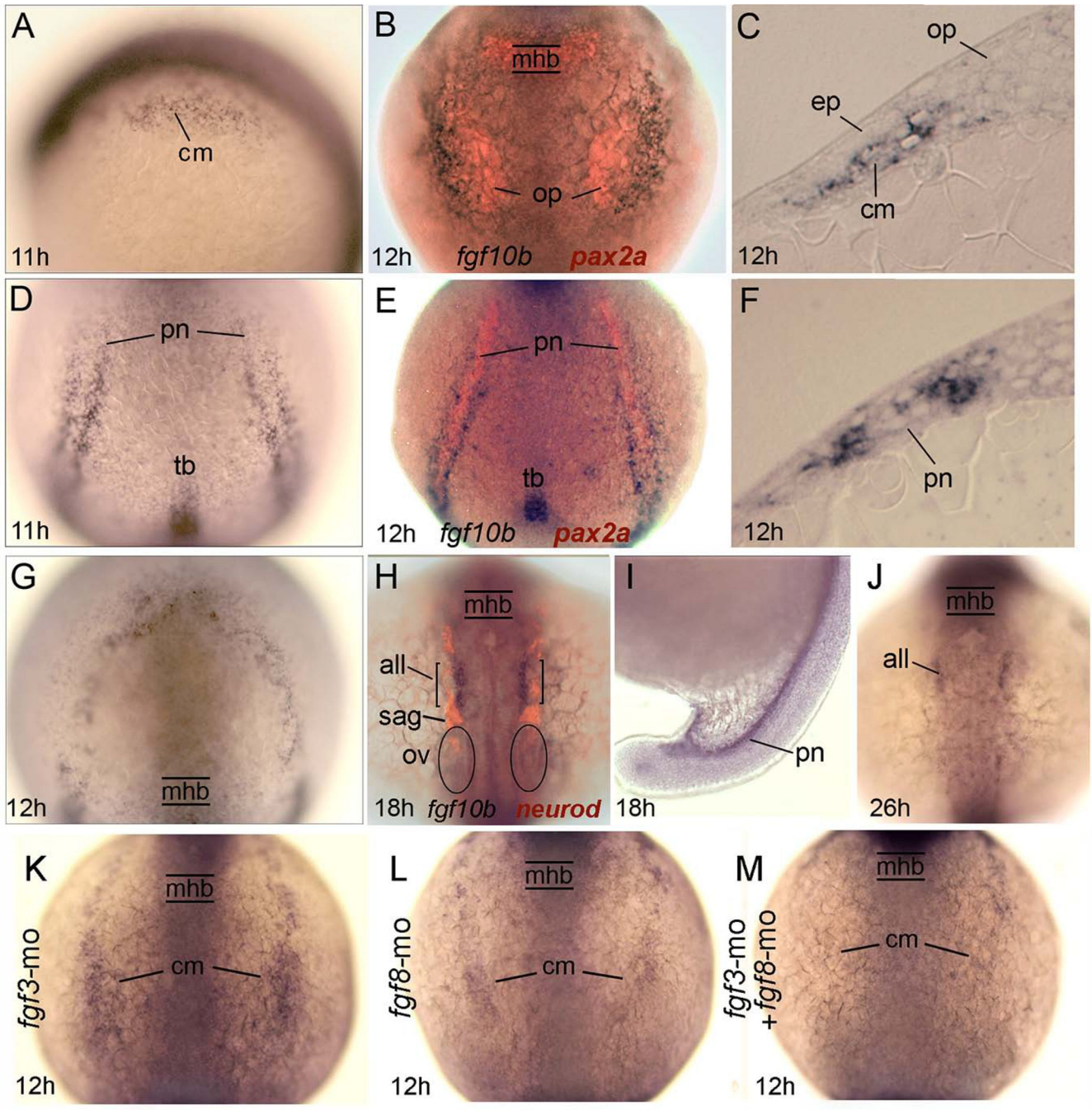

Fig. 1.

Expression and regulation of *fgf10b*. **A–G**: Early expression of *fgf10b* marks mesoderm near the otic/epibranchial domain (A–C), flaking the pronephros (D–F) and surrounding the anterior neural plate (G). Specimens in (B) and (E) also show *pax2a* expression (red) in the otic placode and pronephros, while (C) and (F) show *fgf10b* expression in cross sections. **H–J**: Late expression in the anterior lateral line and pronephros. The specimen in (H) also shows *neurod* expression (red) to reveal neurogenesis in various placodal derivatives. **K–M:** Expression of *fgf10b* in cranial mesoderm appears normal in *fgf3* morphants (K) but is

reduced in *fgf8* morphants (L) and nearly abolished in *fgf3-fgf8* double morphants (M). Abbreviations: all, anterior lateral line; cm, cranial mesoderm; ep, epibranchial placode; mhb, midbrain-hindbrain border. op, otic placode; ov, otic vesicle; pn, pronephros; sag, statoacoustic ganglion; tb, tailbud. Wholemount specimens are shown with dorsal views (anterior to the top) except for (A, I), which are lateral views with dorsal to the right. Cross sections are shown with dorsal to the top.

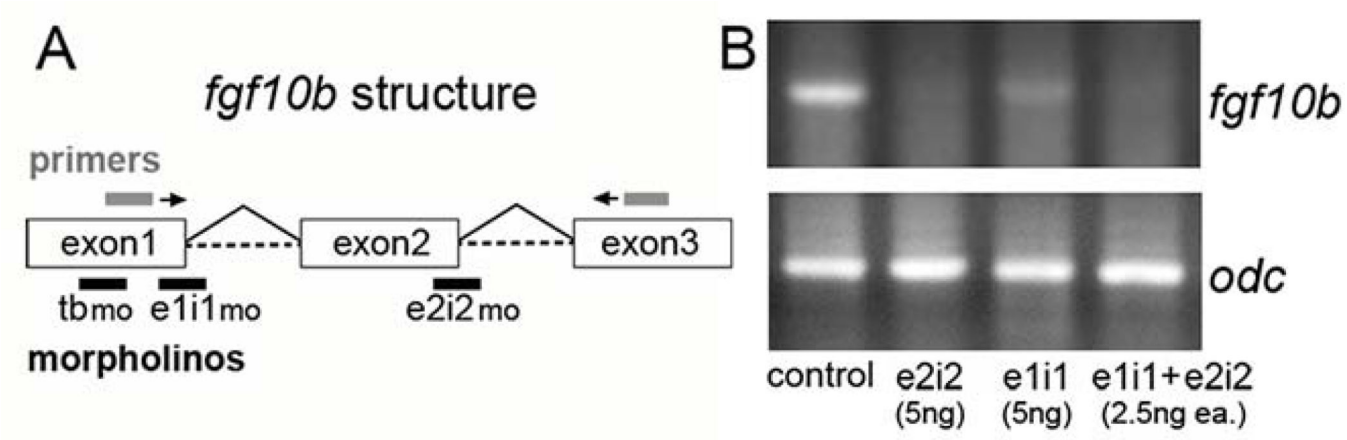

Figure 2.

Efficacy of *fgf10b* knockdown. **A**: Diagram showing the exon/intron structure of the *fgf10b* locus. Above the diagram are primer-binding sites for PCR, and below are target sites for translation-blocking MO (tbmo) and splice-blocking MOs (e1i1mo) and (e2i2mo). **B**: RT-PCR amplification of *fgf10b* mRNA at 12 hpf in control embryos or embryos injected with the indicated mounts of splice-blocking MO. Expression of *ornithine decarboxylase* (*odc*) at 12 hpf serves as a control.

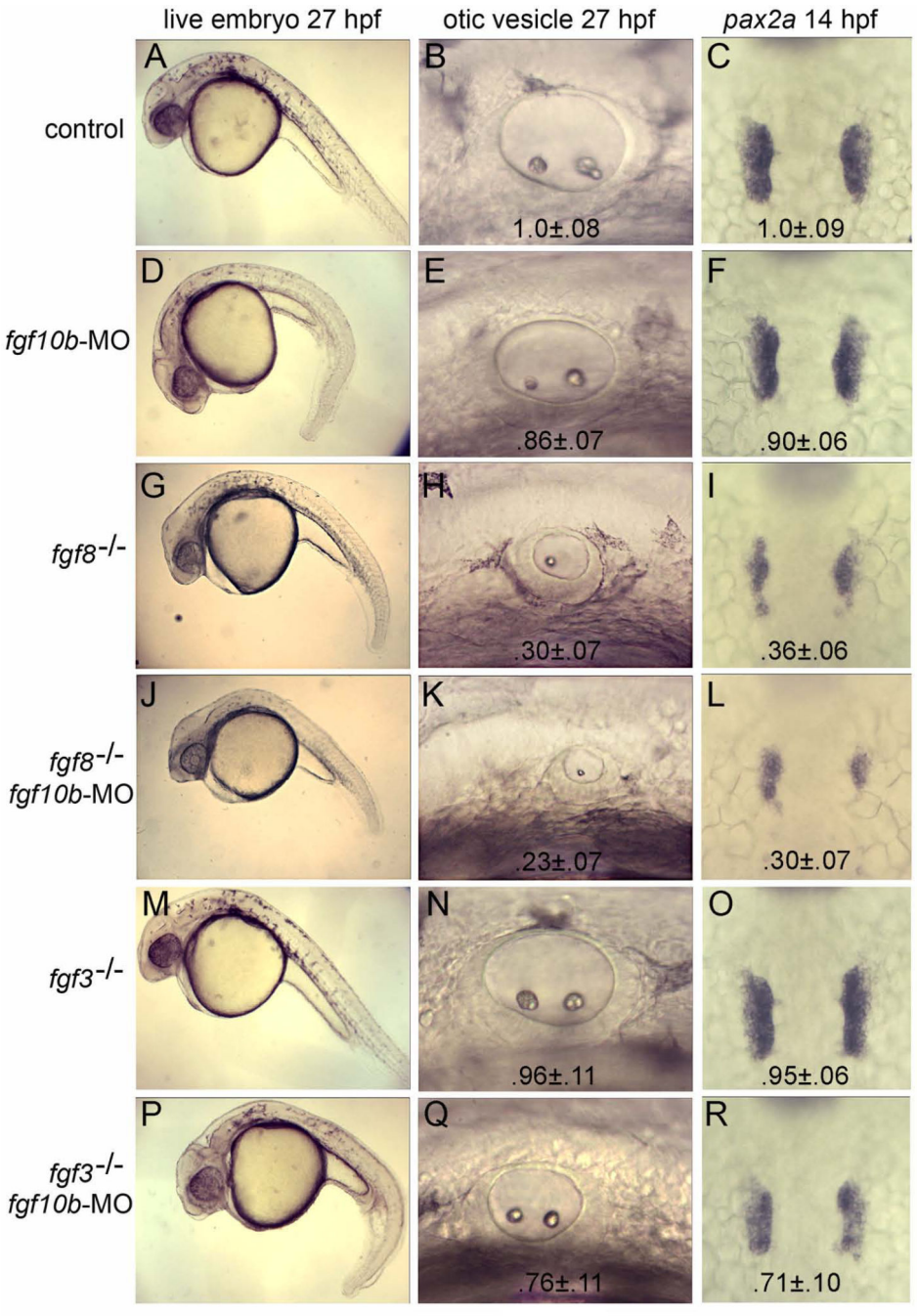

Figure 3.

fgf10b cooperates with *fgf3* and *fgf8* in otic induction. **A–R**: Live specimens at 27 hpf viewed at low magnification to show general morphology and high magnification to show otic vesicles; and dorsal views of in situ hybridizations to visualize *pax2a* in the otic placodes at 14 hpf. Genetic manipulations are indicated down the left side of the figure. Mean surface area (± standard deviation, n≥8) of otic placodes and vesicles, normalized to wild-type control embryos, are indicated for each genotype/knockdown.

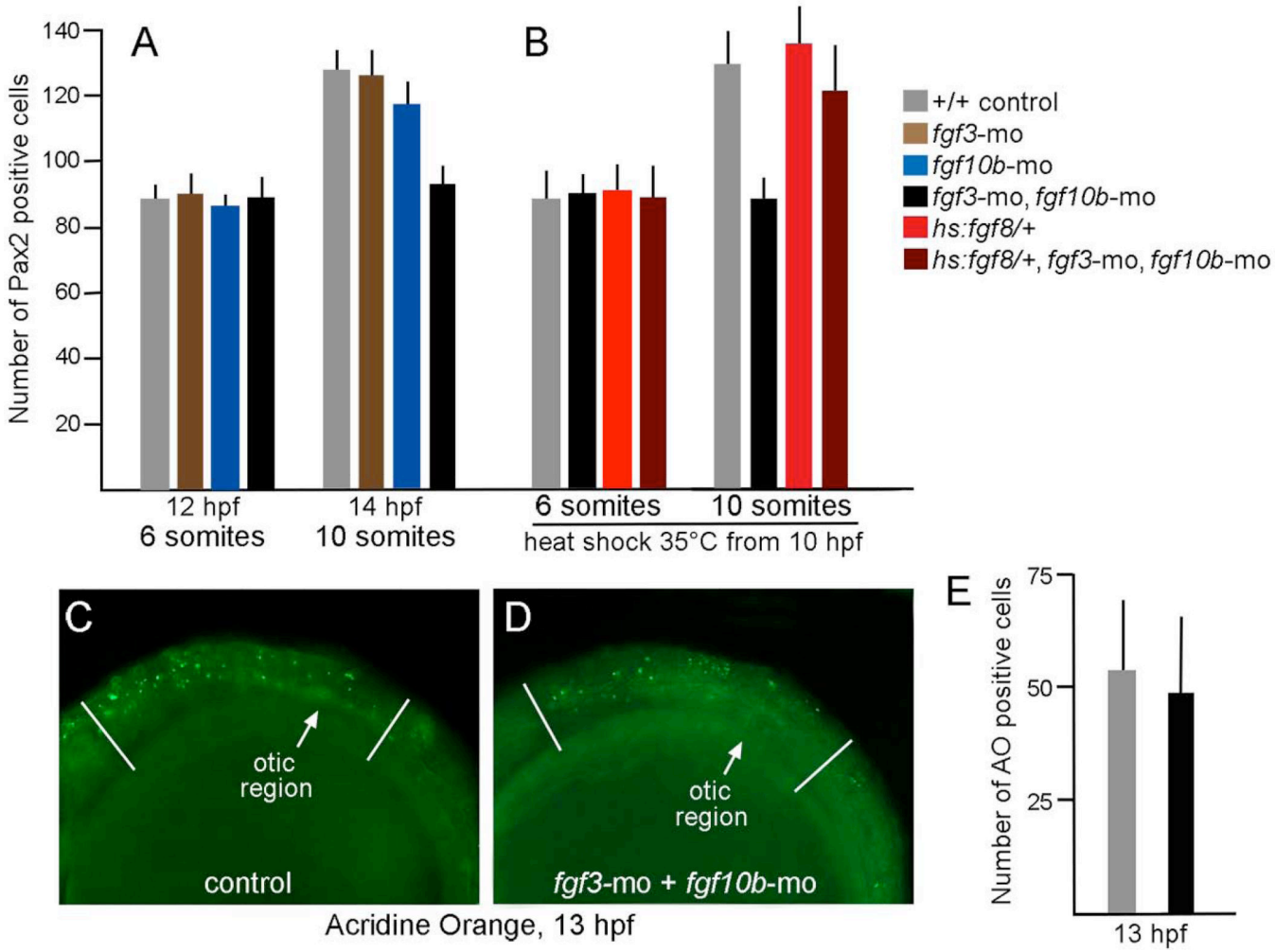

Figure 4.

Otic deficiencies in *fgf3-fgf10b* double morphants and rescue by timed misexpression of *fgf8*. **A–B**: The number of Pax2-expressing cells in the otic vesicle at 12 hpf and 14 hpf in embryos with various genotypes and gene knockdown, as indicated in the color key. Embryos in (B) were incubated at 35°C from 10 hpf until fixation at the 8- or 10-somite stage. Note that incubation at 35°C accelerates development such that these stages occur slightly earlier than normal. **C–D**: Comparison of the number of apoptotic cells stained with acridine orange (AO) in the head between the eye and first somite (marked by white lines), as seen from a lateral view in control embryos (C) or *fgf3-fgf10b* double morphants (D). Data in (E) show means and standard deviations of eight specimens each.

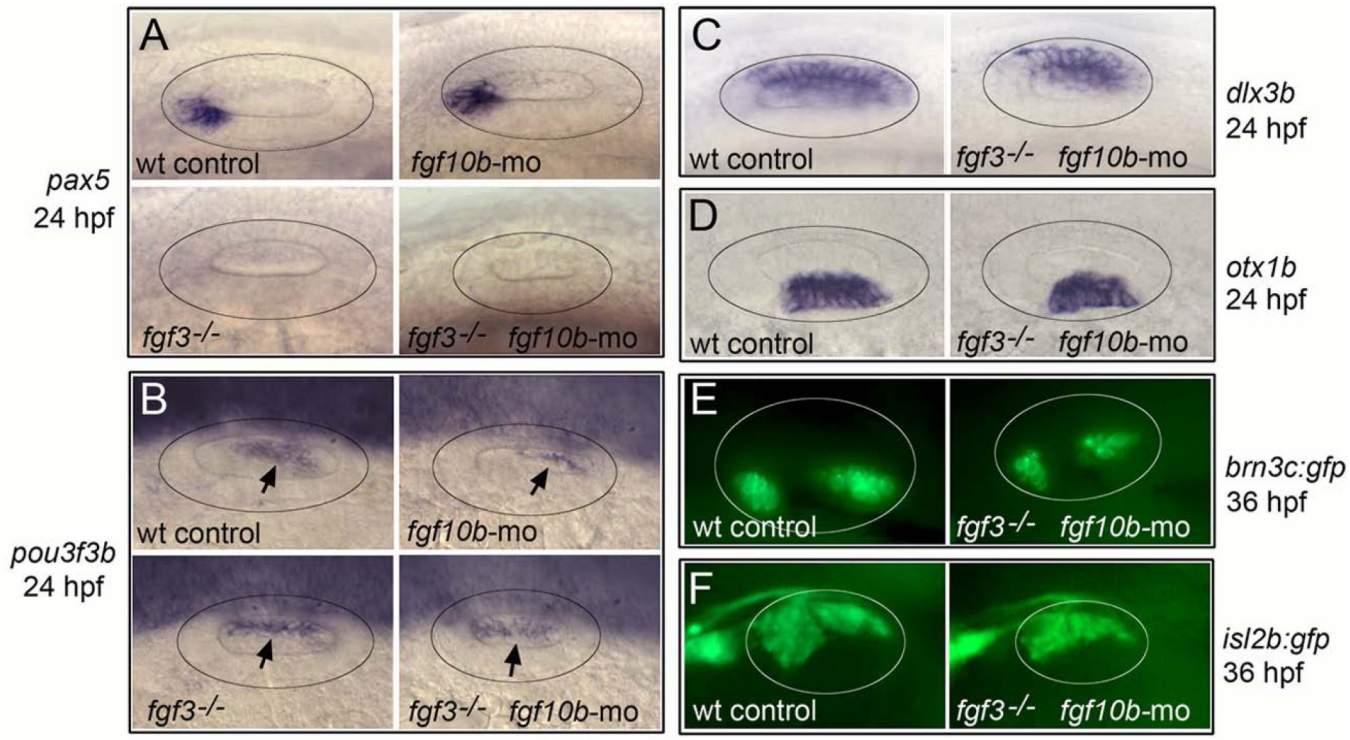

Figure 5.

Effects of *fgf10b* knockdown on otic vesicle patterning. **A–F**: Lateral view (anterior to the left) of the otic vesicle (circled) at 24 hpf (A–D) and 36 hpf (E–F) labeled for the indicated genes. Arrows in (B) indicate the otic domain of *pou3f3b.*

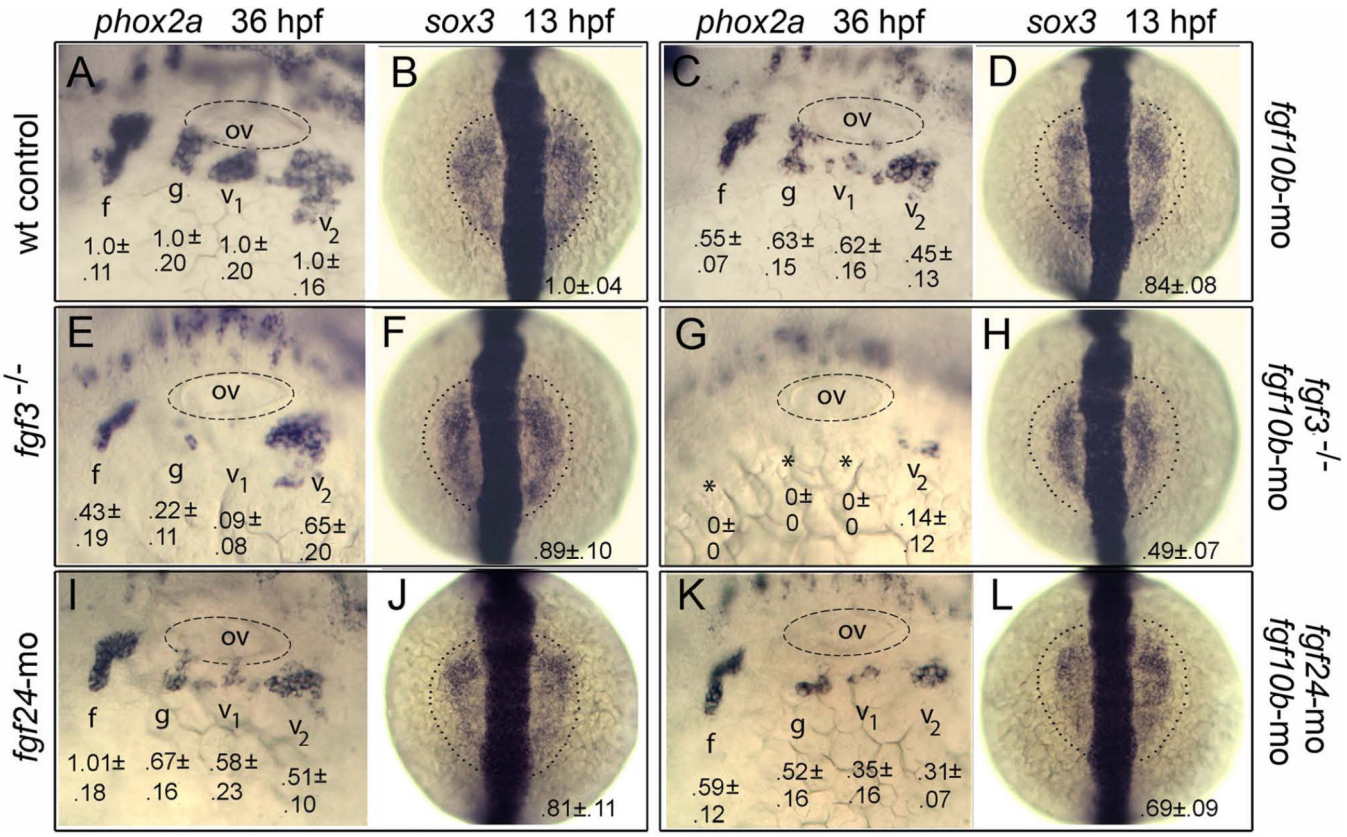

Figure 6.

fgf10b cooperates with *fgf3* and *fgf24* in epibranchial induction. **A–L**: Lateral views (anterior to the left) of *phox2a* expression in epibranchial ganglia at 36 hpf; and dorsal views (anterior to the top) of *sox3* expression at 13 hpf (normal boundaries of the control are outlined). Genetic manipulations are indicated along the sides. Positions of the otic vesicle (ov) and facial (f), glossopharyngeal (g) and vagal ganglia (v1 and v2) are indicated. Mean surface areas (± standard deviation, n≥8), normalized to wild-type control embryos, are indicated for each structure.

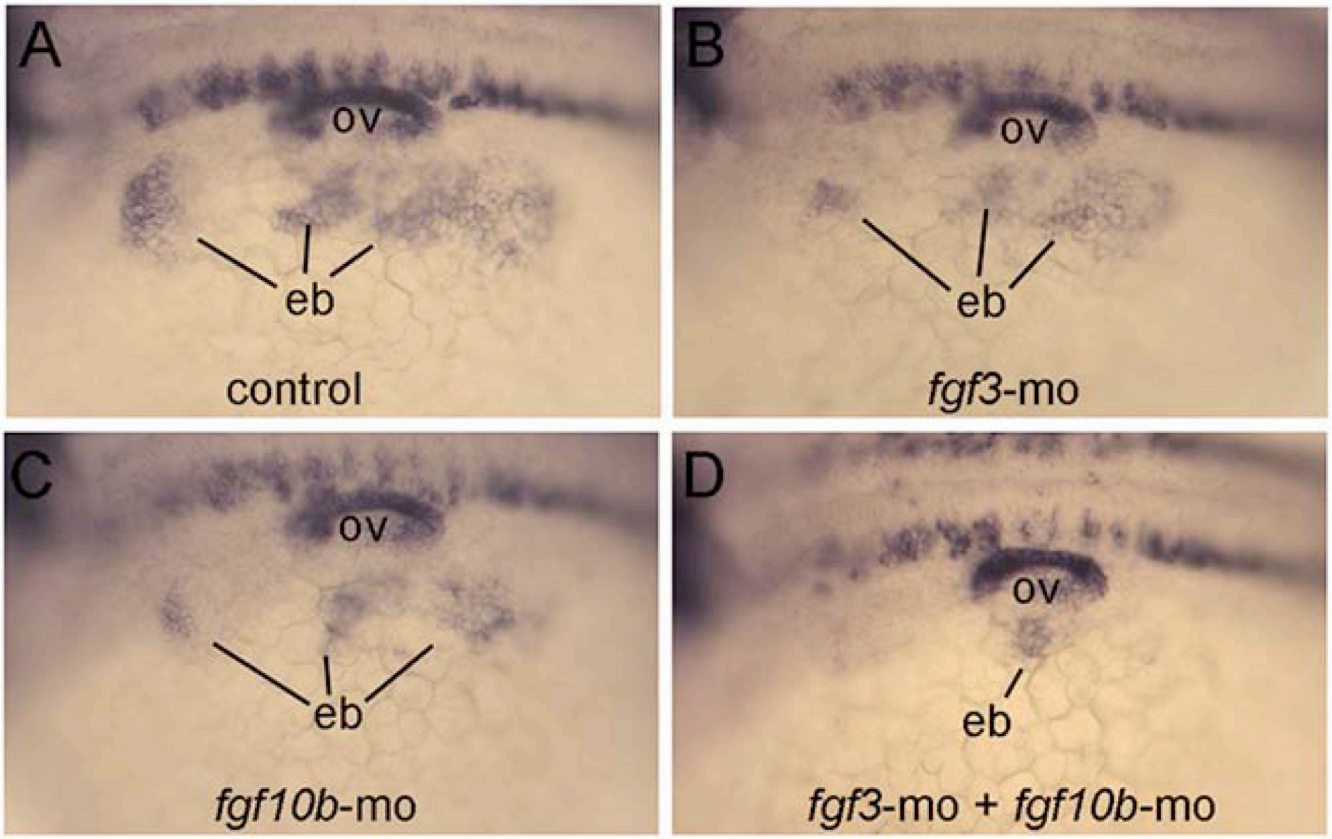

Figure 7.

Loss of epibranchial expression of *pax2a* in *fgf3-fgf10b* deficient embryos. **A–D**: Lateral views (anterior to the left) showing expression of *pax2a* in the otic vesicle (ov) and nascent epibranchial placode (eb) at 24 hpf. Compared to a control embryo (A), knockdown of *fgf3* (B) or *fgf10b* (C) causes moderate deficiencies in epibranchial placodes, whereas knockdown of both *fgf3* and *fgf10b* nearly abolishes the epibranchial domain (D).

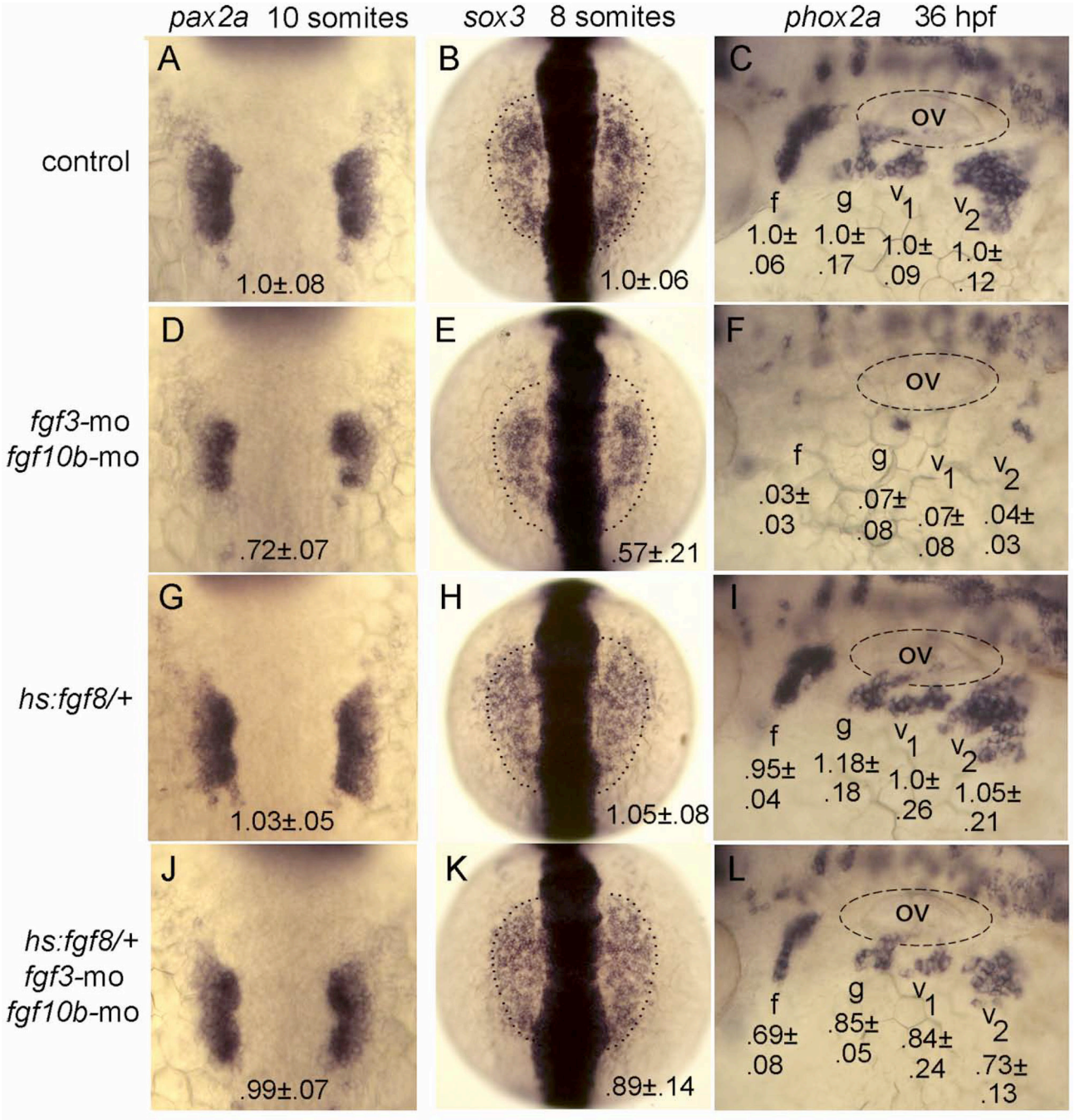

Figure 8.

Rescue of epibranchial development in *fgf3-fgf10b* deficient embryos by timed misexpression of *fgf8*. **A–L**: Dorsal views (anterior to the top) of *pax2a* expression at the 10-somite stage and *sox3* expression at the 8-somite stage (normal boundaries of the control are outlined), and lateral views (anterior to the left) of *phox2a* expression at 36 hpf in embryos incubated at 35°C from 10 hpf until the 8-somite stage (for *sox3*) or the 10-somite stage (for *pax2a* and *phox2a*). Genetic manipulations are indicated along the left side. Positions of the otic vesicle (ov) and facial (f), glossopharyngeal (g) and vagal ganglia (v1 and v2) are

indicated. Mean surface areas (± standard deviation, n≥8), normalized to wild-type control embryos, are indicated for each structure

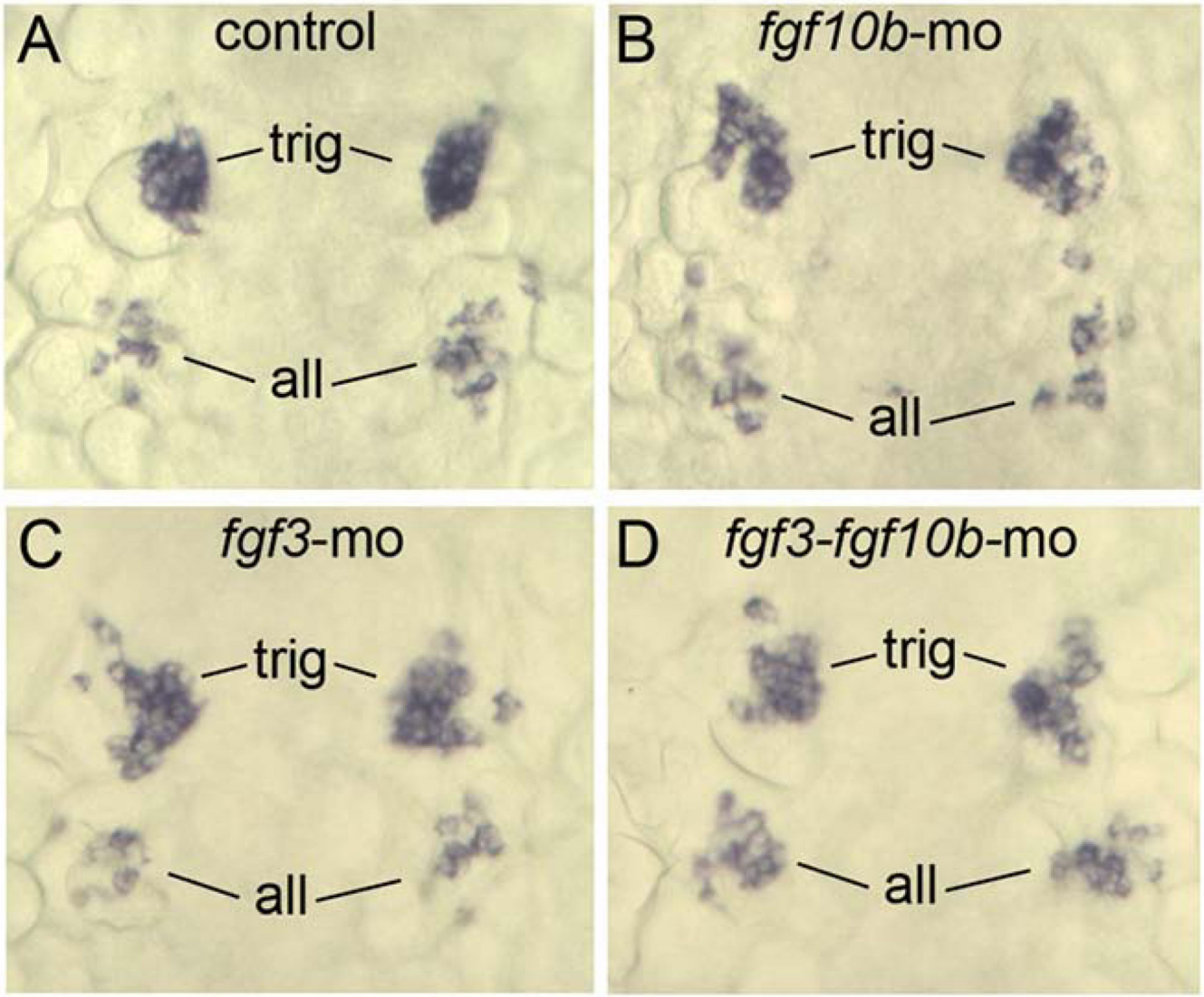

Figure 9.

fgf10b is not required for development of other cranial placodes. **A–D**: Dorsal views (anterior to the top) showing expression of *neurod* in nascent trigeminal (trig) and anterior lateral line (all) placodes at 14 hpf in a control embryo (A), *fgf10b* morphant (B), *fgf3* morphant (C) and *fgf3-fgf10b* double morphant.

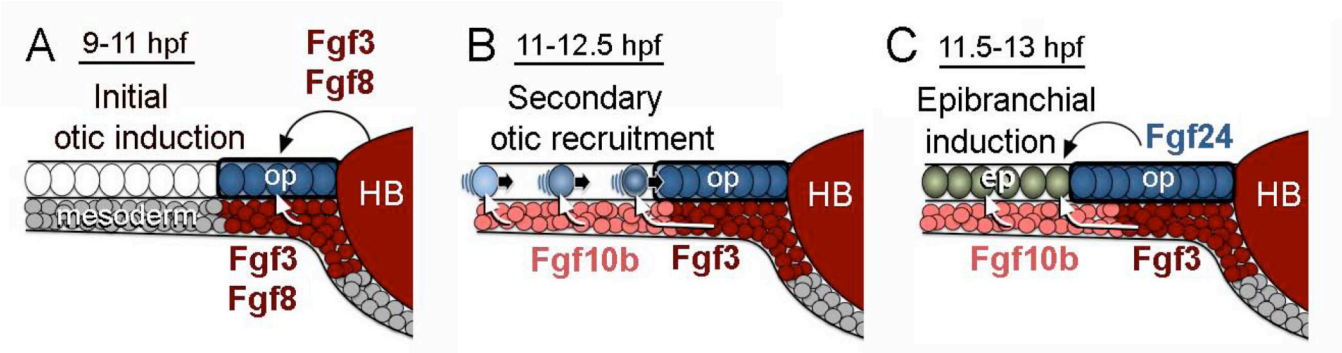

Figure 10.

A network of Fgf ligands regulates otic-epibranchial induction. **A**: Initial otic induction is mediated by Fgf3 and Fgf8 from the hindbrain (HB) and sub-otic mesoderm. **B**: During secondary otic recruitment, cells converging from more lateral regions initially encounter mesodermal Fgf10b followed by Fgf3. Newly recruited cells continue to join the otic placode through 12.5 hpf (Bhat et al., 2010). **C**: In a final phase, epibranchial fates are induced by a combination of mesodermal Fgf10b and Fgf3 and otic Fgf24. Cells in the facial placode are induced first, followed by cells in more posterior epibranchial tissue (Nechiporuk et al., 2007).